Supporting Information

Structure-based principles underlying ligand recognition of xanthine-II riboswitch

Xiaochen Xu[1,2], Mengqi He[1], Xiaoqing Tai[1], Qianyu Ren[3], Xin Shen[1], Chunyan Li[1], Aiming Ren[1*]

[1]Department of Cardiology, Second Affiliated Hospital of Zhejiang University School of Medicine, Life Sciences Institute, Zhejiang University, Hangzhou 310058, China;

[2]Department of Hematology, The Eighth Affiliated Hospital, Sun Yat-Sen University, Shenzhen, Guangdong 518033, China;

[3]Agricultural College, Yangzhou University, Yangzhou 225009, China

[*]Corresponding authors (Aiming Ren, email: aimingren@zju.edu.cn).

Contents

Supplementary Tables

Table S1 Crystallographic statistics of xanthine-II riboswitches

	Xanthine-II riboswitch bound to Xanthine	Xanthine-II-ML2/3 bound to Xanthine
Data collection		
Space group	*P* $2_12_12_1$	*P* $2_12_12_1$
a, b, c (Å)	26.6, 115.8, 126.8	26.4, 117.8, 125.6
α, β, ϒ (º)	90,90,90	90,90,90
Wavelength(Å)	0.978	1.009
Resolution (Å)	85.5-2.1(2.2-2.1)	62.8.0-2.5(2.6-2.5)
R_{pim}	0.02(0.3)	0.03(0.3)
$I/\delta I$	19.5(2.4)	22.3(2.8)
Completeness (%)	97.2 (100.0)	97.8 (99.9)
Multiplicity	12.4 (12.9)	12.2 (13.0)
$CC_{1/2}$	1.0 (0.8)	1.0(0.9)
Refinement		
Resolution (Å)	30.6-2.1(2.1-2.1)	43.0-2.5(2.6-2.5)
No.reflections	24648	14424
R_{work}/R_{free} (%)	21.9/25.4	23.3/26.8
No. of atoms		
RNA	2986	2996
Ligand	22	22
Mg^{2+}	15	24
Water	110	85
B-factors(Å^2)		
RNA	52.6	56.9
Ligand	34.8	35.3
Mg^{2+}	49.7	50.8
Water	45.6	52.8
R.m.s deviations		
Bond lengths (Å)	0.005	0.002
Bond angles (º)	1.1	0.6

*Values for the highest-resolution shell are in parentheses.

Table S2 Thermodynamic parameters of ligand binding to xanthine-II riboswitch determined by isothermal titration calorimetry (ITC).

RNA	Ligand	1H [kcal/mol]	-T1S [kcal/mol]	∆ G [kcal/mol]	∆ ∆ G [kcal/mol]	N[a]	K_d[b] [μM]	c-value	K_d[c] (Mean) [μM]
Xanthine-II riboswitch from *P. beijingensis*	Na Xanthine	-15.6±0.1 -16.4±0.4 -18.2±1.0	8.9 9.6 11.7	-6.7 -6.8 -6.4	--	0.6±1.3e^{-3} 0.6±6.3e^{-3} 0.6±1.3e^{-2}	12.1±0.3 9.9±1.11 19.7±4.2	8.3 10.1 5.1	13.9±5.1
Xanthine-II-ML2/3	Na Xanthine	-18.7±0.1 -18.5±0.2 -18.5±0.1	12.4 12.4 12.3	-6.3 -6.1 -6.2	-0.4	0.9±4.6e^{-3} 0.9±6.3e^{-3} 0.9±4.4e^{-3}	25.2±0.7 32.4±1.3 31.3±0.9	4.0 3.1 3.2	29.6±3.9
Xanthine-II-ML2/3 (pH 6.0)	Na Xanthine	-15.3±0.1	9.0	-6.3	-0.3	1.0±9.4e^{-2}	24.7±1.3	4.0	
Xanthine-II-ML2/3 (pH 8.5)	Na Xanthine						N.D.[d]		
Xanthine-II-ML2/3	8-azaxanthine						N.D.		
Xanthine-II-ML2/3	Uric acid						N.D.		
Xanthine-II-ML2/3	Hypoxanthine						N.D.		
Xanthine-II-ML2/3	guanine						N.D.		
Xanthine-II-ML2/3	Adenosine						N.D.		
Xanthine-II-ML2/3	Adenine						N.D.		
Xanthine-II-ML2/3	Inosine						N.D.		
Xanthine-II-ML2/3	guanosine			-			N.D.		
Xanthine-II-ML2/3	2'-dG						N.D.		
Xanthine-II-ML2/3-U8C	Na Xanthine						N.D.		
Xanthine-II-ML2/3-A9C	Na Xanthine						N.D.		
Xanthine-II-ML2/3-A10C	Na Xanthine						N.D.		
Xanthine-II-ML2/3-	Na Xanthine						N.D.		

A19C/U20C									
Xanthine-II-ML2/3-G23C/G24C	Na Xanthine						N.D.		
Xanthine-II-ML2/3-G32C	Na Xanthine						N.D.		
Xanthine-II-ML2/3-U33A	Na Xanthine						N.D.		
Xanthine-II-ML2/3-G37U	Na Xanthine						N.D.		
Xanthine-II-ML2/3-G62C	Na Xanthine						N.D.		
Xanthine-II-ML2/3-C64G	Na Xanthine						N.D.		

[a] N, the stoichiometric ratio of ligand to RNA.
[b] The binding disassociation parameter fitted for each independent titration.
[c] Reported error is the standard deviation of three independent experiments.
[d] N.D. refers to no detectable interaction under the experiment conditions.
All experiments were performed in a buffer containing 50 mM HEPES pH7.5, 50 mM KCl and 10 mM $MgCl_2$ expect special label.

Supplementary Figures

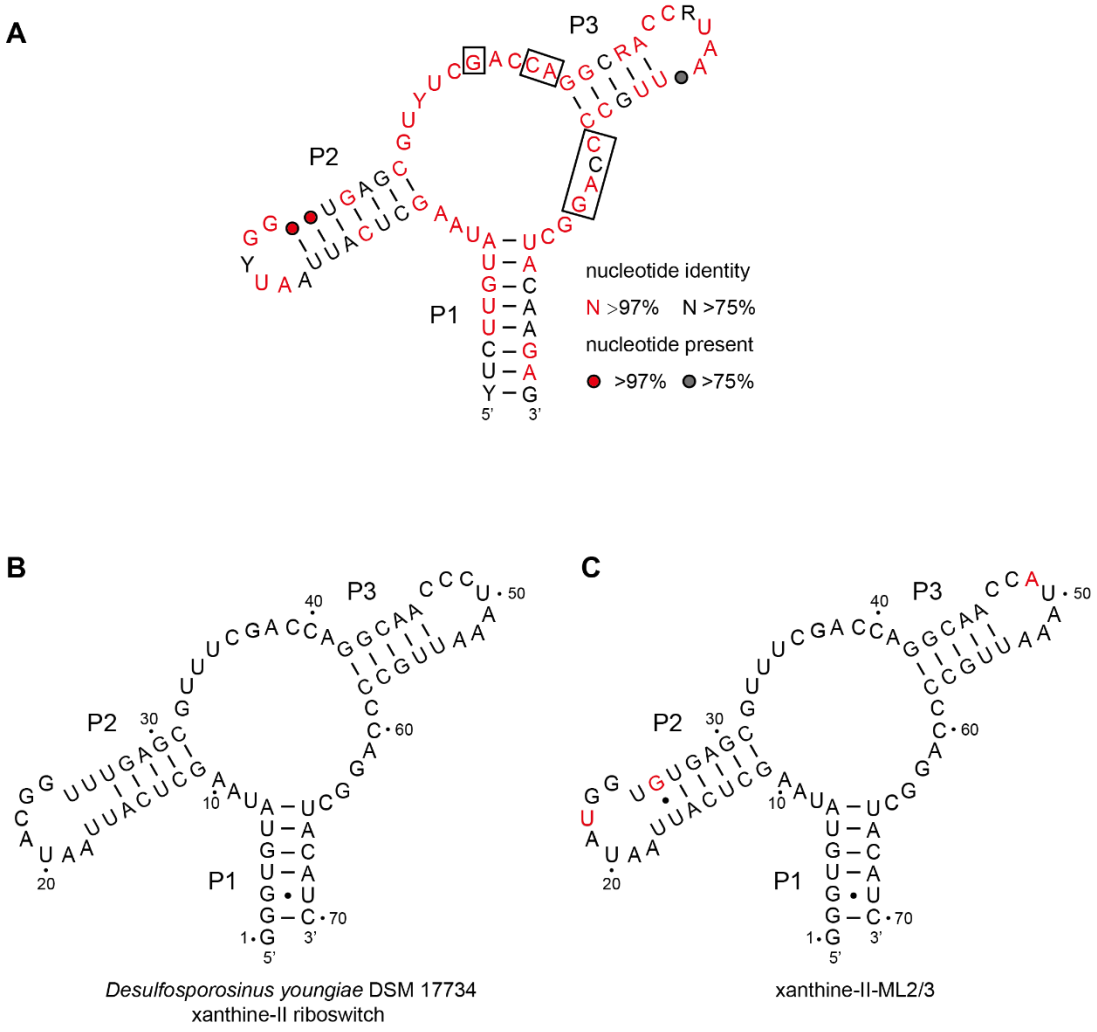

Figure S1. Secondary structure of xanthine-II riboswitch. A, Consensus motif of xanthine-II riboswitch according to phylogenetic sequence analysis (Hamal Dhakal et al., 2022). The highly conserved nucleotides are labelled in red, and nucleotides different from guanine-I riboswitch are labelled by black rectangle. **B,** Secondary structure of *P.beijingensis* xanthine-II riboswitch. **C,** Secondary structure of xanthine-II-ML2/3.

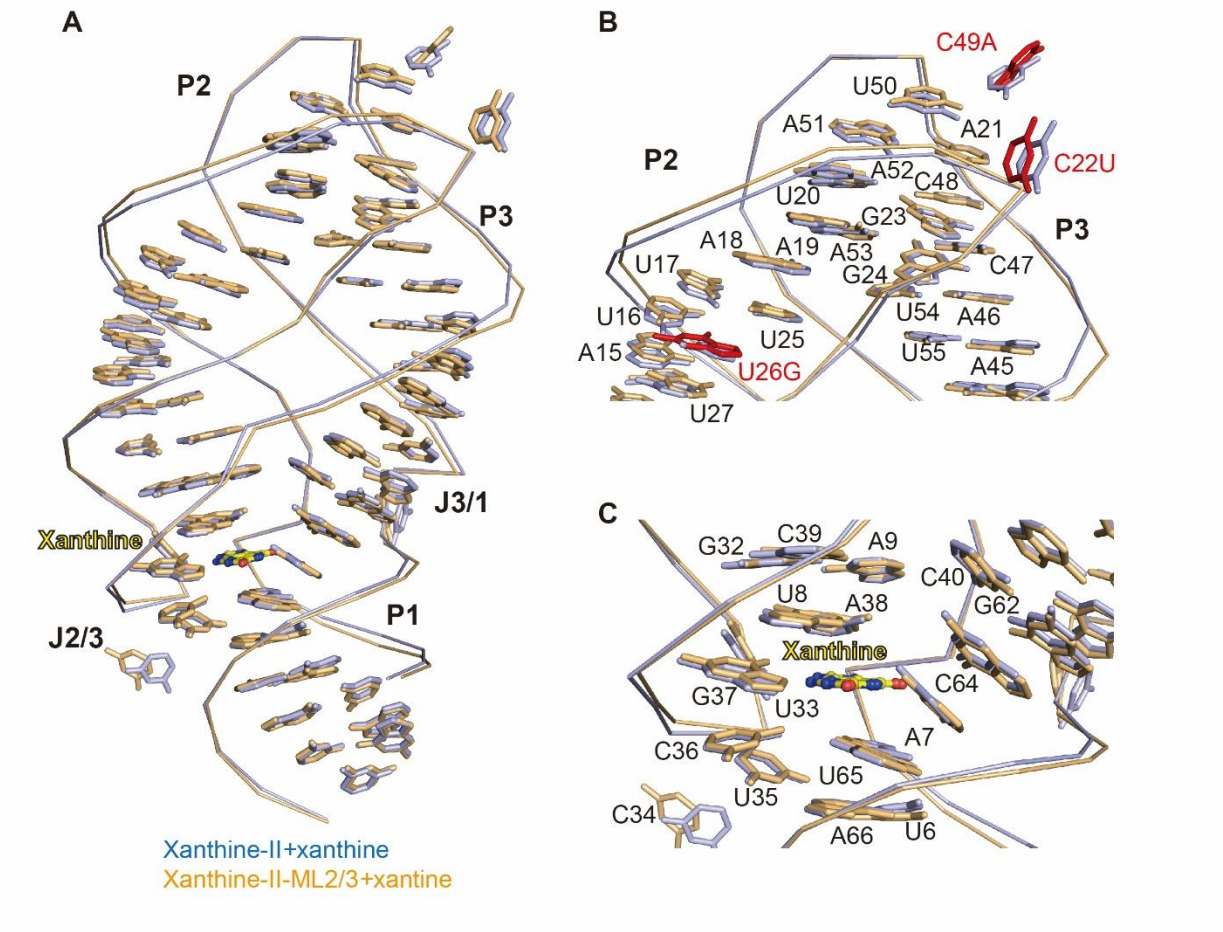

Figure S2. Tertiary structures alignments of *P.beijingensis* xanthine-II riboswitch and xanthine-II-ML2/3. A, Overall structures alignment of *P.beijingensis* xanthine-II riboswitch and xanthine-II-ML2/3. **B,** Alignment of the long-distance interaction between L2 and L3 of *P.beijingensis* xanthine-II riboswitch and xanthine-II-ML2/3. **C,** Binding pockets alignment of *P.beijingensis* xanthine-II riboswitch and xanthine-II-ML2/3.

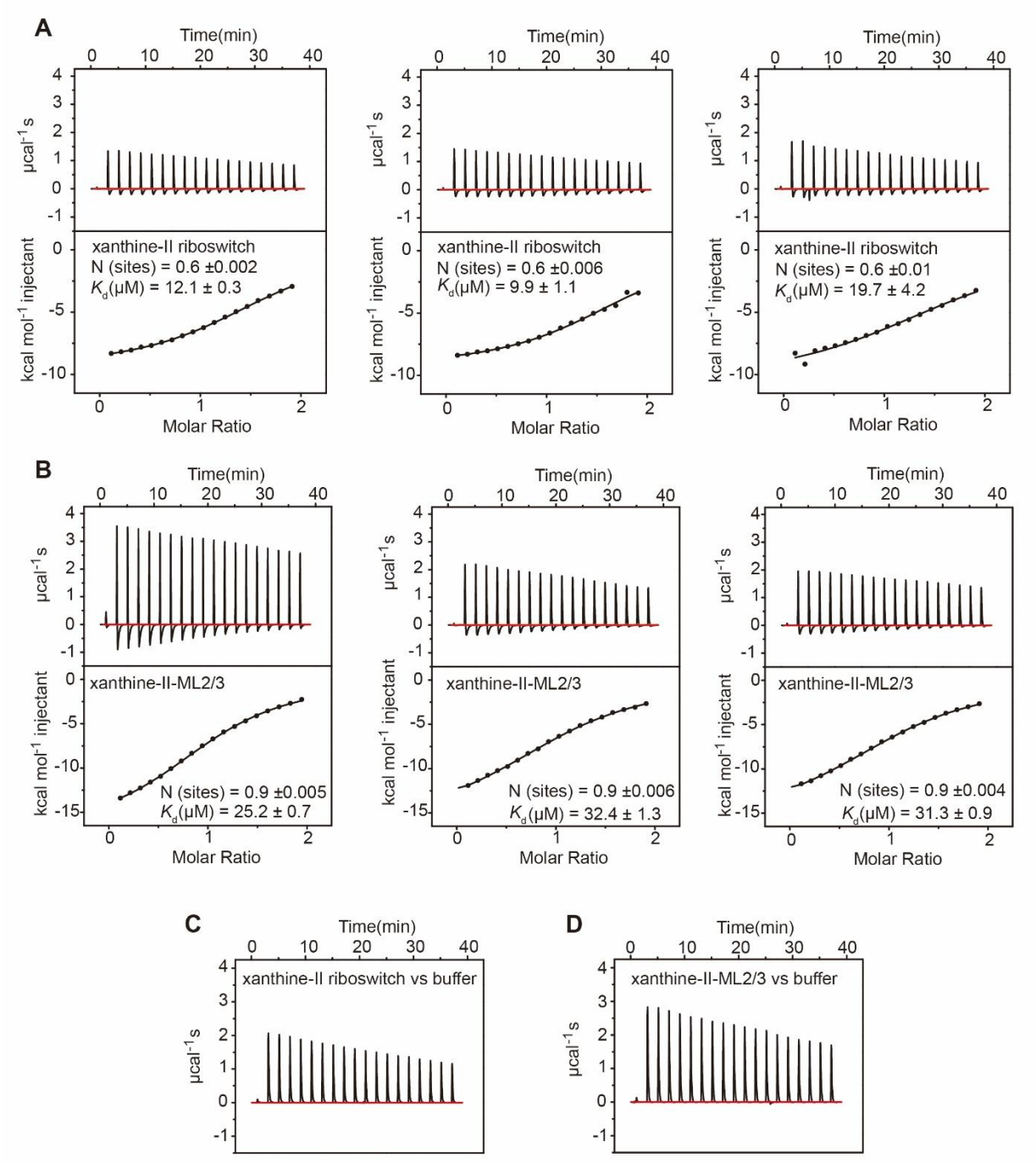

Figure S3. Isothermal titration calorimetry (ITC) of xanthine-II riboswitch bound to xanthine. A, Three independent ITC titration replicates of the *P.beijingensis* xanthine-II riboswitch with xanthine. **B,** Three independent ITC titration replicates of the xanthine-II-ML2/3 with xanthine. **C,** ITC heat plot of the *P.beijingensis* xanthine-II riboswitch titrating to buffer. **D,** ITC heat plot of xanthine-II-ML2/3 titrating to buffer.

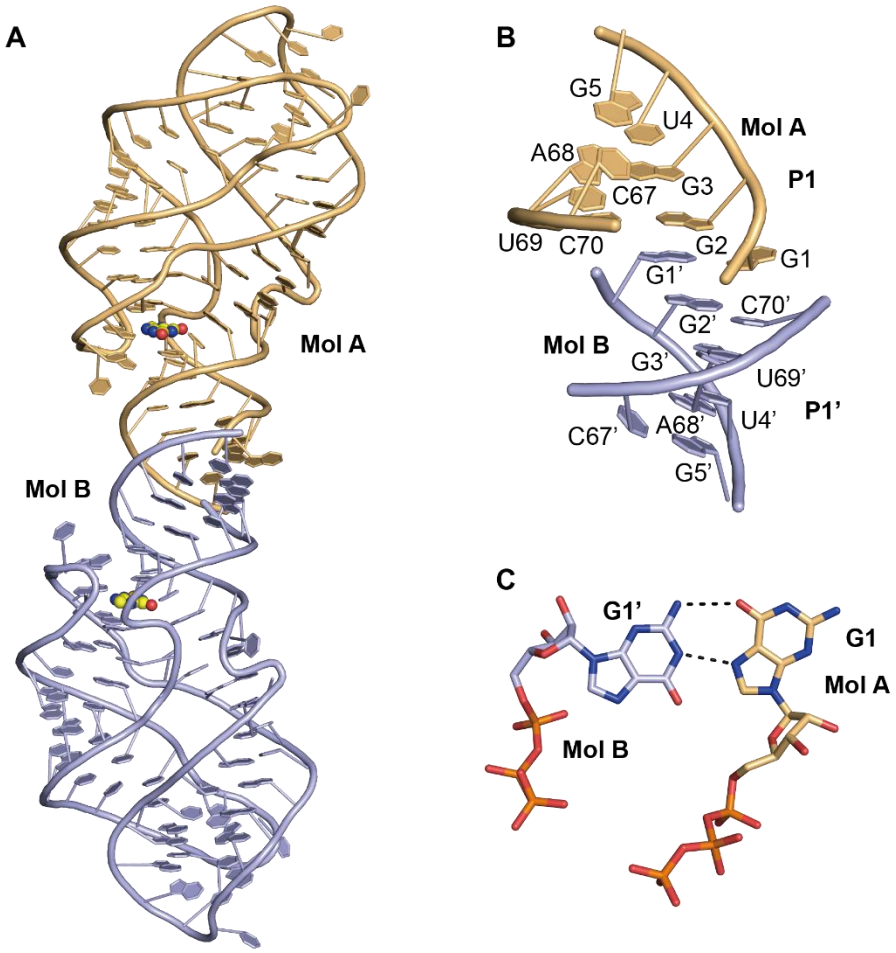

Figure S4. Crystal packing interactions of xanthine-II riboswitch molecules. A, One asymmetric unit of xanthine-II riboswitch contains two end-to-end packing RNA molecules, Mol A (light orange) and Mol B (light blue). **B,** Mol A and Mol B adopt end-to-end stacking interaction. **C,** A close-up view of the packing interaction between Mol A and Mol B. The Hoogsteen edge of the overhang G1 in Mol A forms two hydrogen bonds with the Watson-Crick edge of the overhang G1' in Mol B.

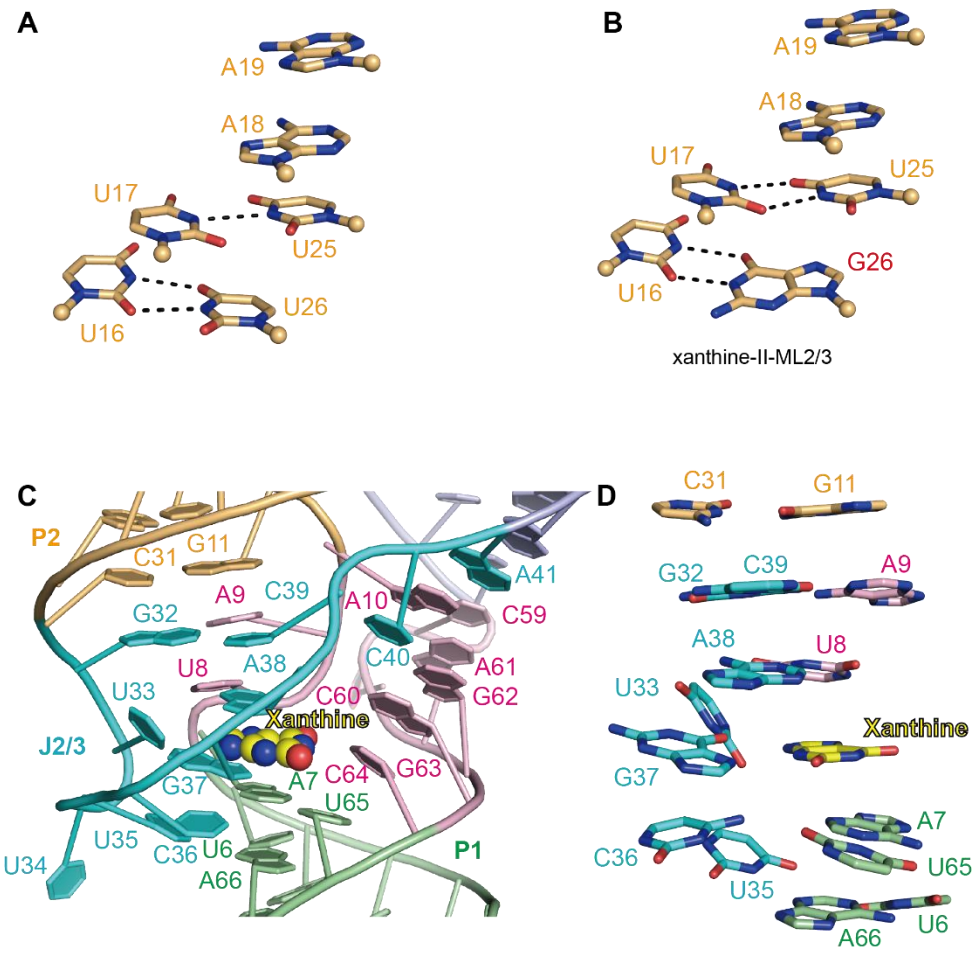

Figure S5. Structural details of the long-distance interaction in xanthine-II riboswitch. A, A close-up view of the long-distance interactions between U16, U17 from L2 and U25, U26 from L3 in xanthine-II riboswitch. **B,** A close-up view of the long-distance interactions between U16, U17 from L2 and U25, G26 from L3 in xanthine-II-ML2/3. **C,** Structural details of the long-distance interaction between J1/2, J2/3 and J3/1. **D,** Nucleotides alignment of J1/2 and J2/3 stacking between stem P1 and P2 in xanthine-II riboswitch.

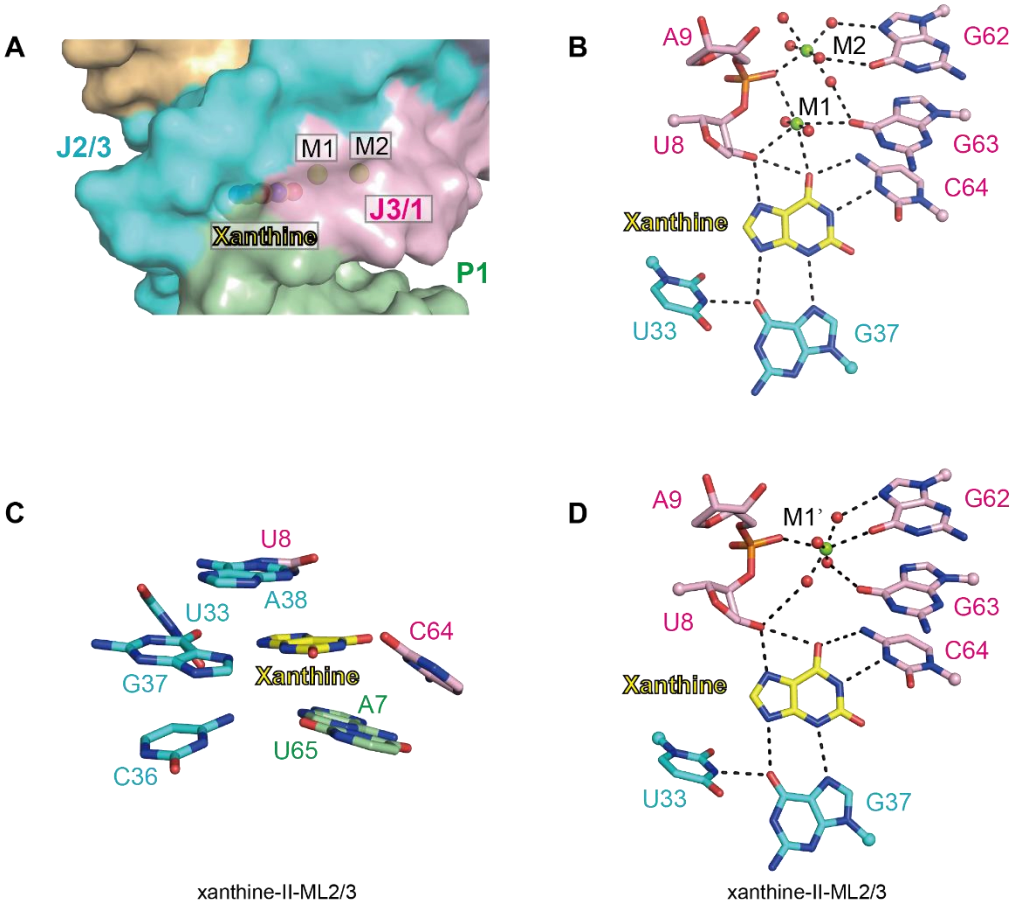

Figure S6. Metal ions along binding pocket of xanthine-II riboswitch. A, surface representation of the binding pocket of xanthine-II riboswitch. Xanthine (shown in sphere) is bound in the junction region and two metal ions locate beside xanthine. **B,** M1 and M2 are located between the main chain of U8-A9 and the bases of G62-G63. M1 forms inner-sphere coordination with O6 of xanthine directly. **C,** Binding pocket of xanthine-II-ML2/3. Xanthine pairs with G37 and C64, and is sandwiched by base pair U8-A38 and base triple A7-C36-U65. **D,** Metal ion M1' locates beside xanthine in xanthine-II-ML2/3.

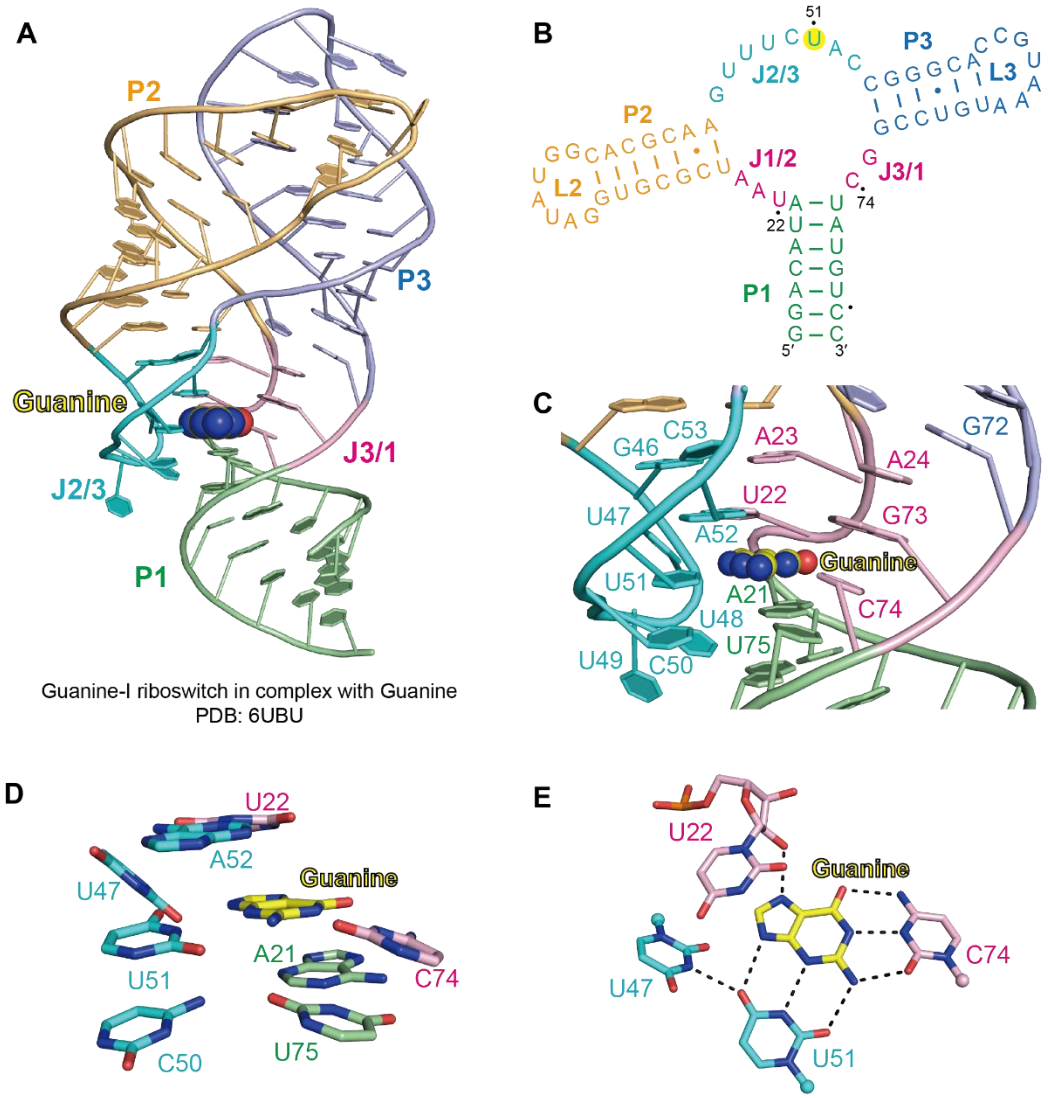

Figure S7. Tertiary structure of guanine-I riboswitch. A, Cartoon representation of the tertiary structure of guanine-I riboswitch bound to guanine (shown in spheres) (PDB:6UBU). **B,** Secondary structure of guanine-I riboswitch, same colour code as the cartoon representation. **C,** structure details of the junction regions in guanine-I riboswitch. **D,** Binding pocket of guanine-I riboswitch. Guanine pairs with U51 and C74, and is sandwiched by base pair U22-A52 and base triple A21-C50-U75. **E,** The Watson-Crick edge of C74 forms three hydrogen bonds with the Watson-Crick edge of guanine, the Watson-Crick edge of U51 forms three hydrogen bonds with the minor groove edge of guanine. And the sugar of U22 forms a hydrogen bond with the N7 of guanine.

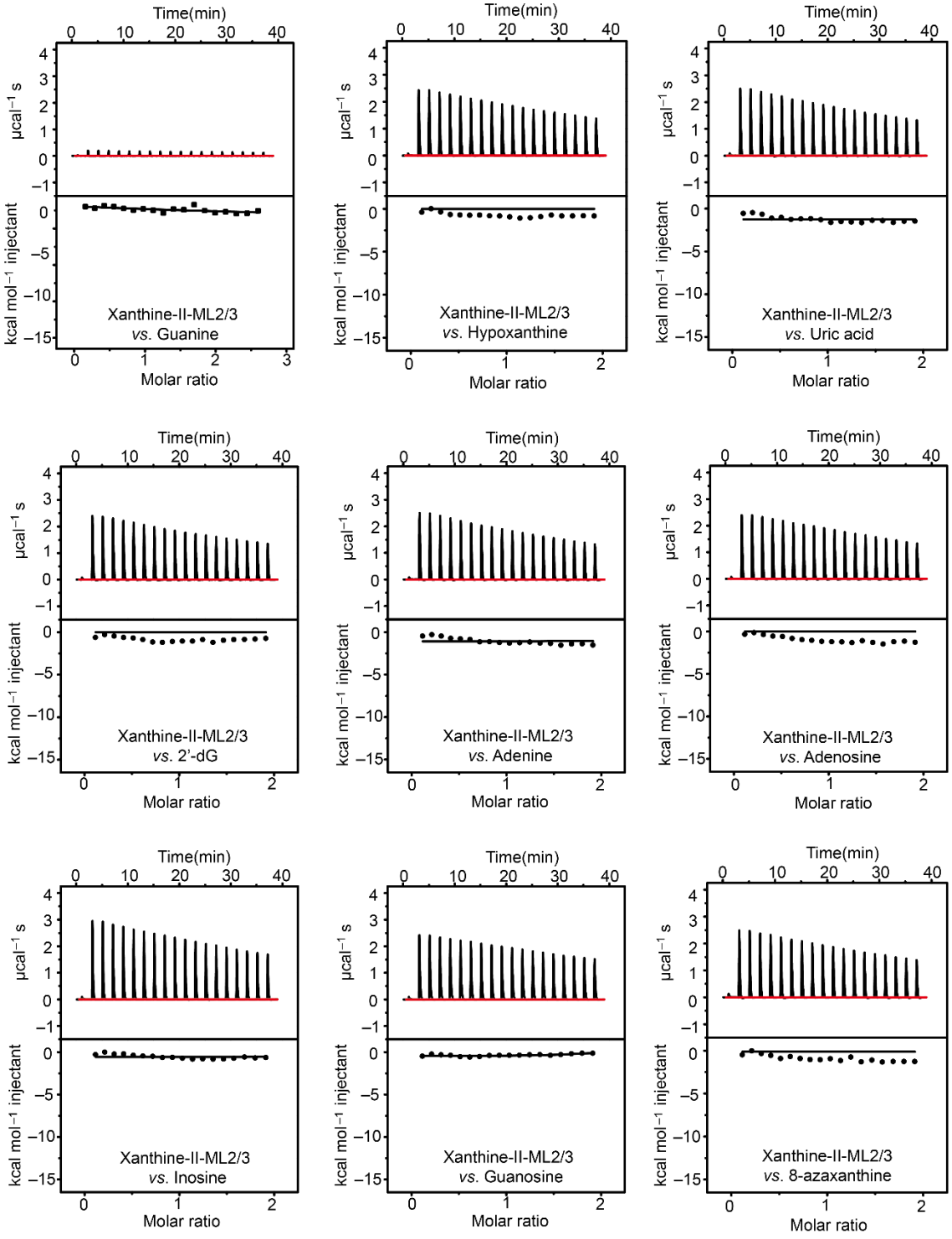

Figure S8. Independently ITC experiments of xanthine-II riboswitch bound to purine molecules. ITC binding curves of xanthine-II riboswitch bound to guanine, hypoxanthine, uric acid, 2'-dG, adenine, adenosine, inosine, guanosine and 8-azaxanthine, respectively. All titrations were performed at 25 °C in 50 mmol L^{-1} HEPES pH7.5, 50 mmol L^{-1} KCl and 10 mmol L^{-1} $MgCl_2$. For K_d, N parameters and c-values see Table S2 in supporting information.

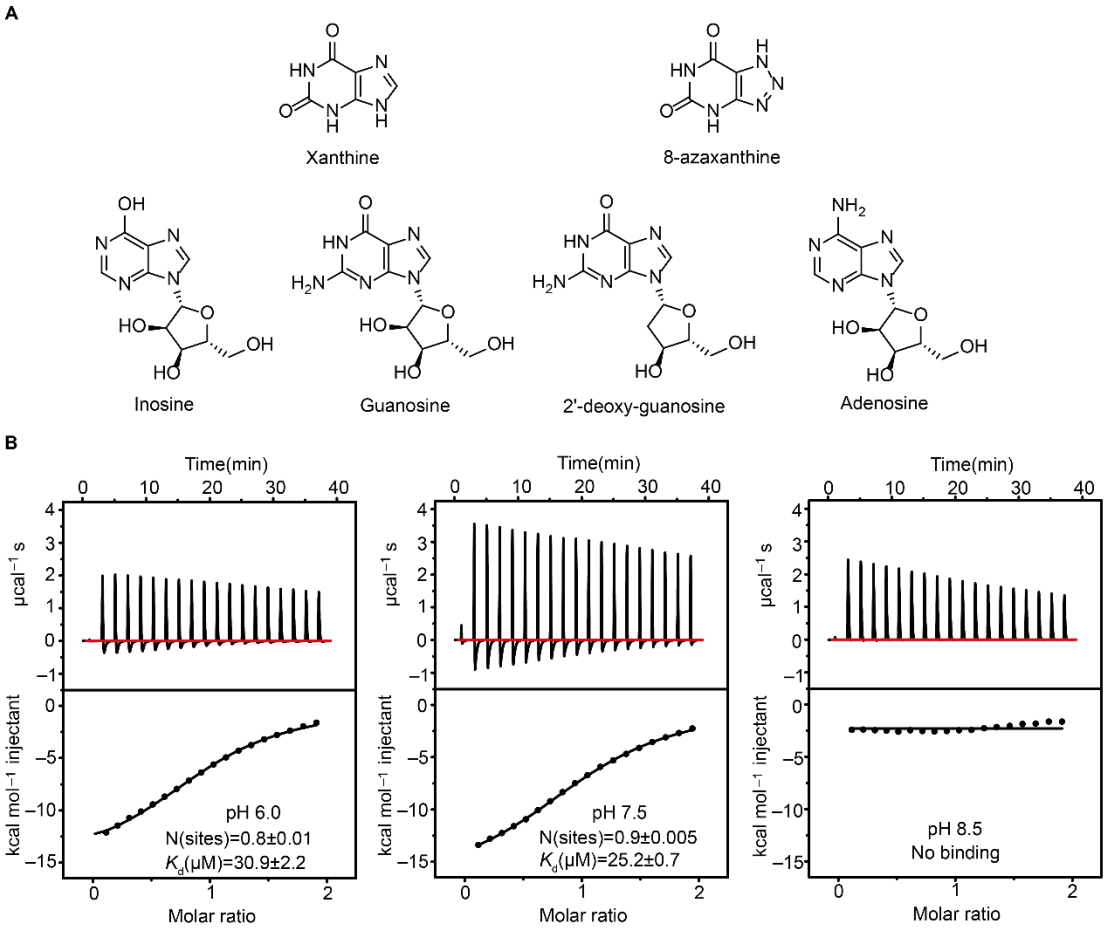

Figure S9. The pH-dependence ITC experiments of xanthine-II riboswitch binding to xanthine. A, chemical structure of xanthine, uric acid, 2'-dG, adenosine, inosine, guanosine and 8-azaxanthine. **B,** ITC heat plot of the xanthine-II riboswitch binding to xanthine in pH 6.0, 7.5 and 8.5. For K_d, N parameters and c-values see Table S2 in supporting information.

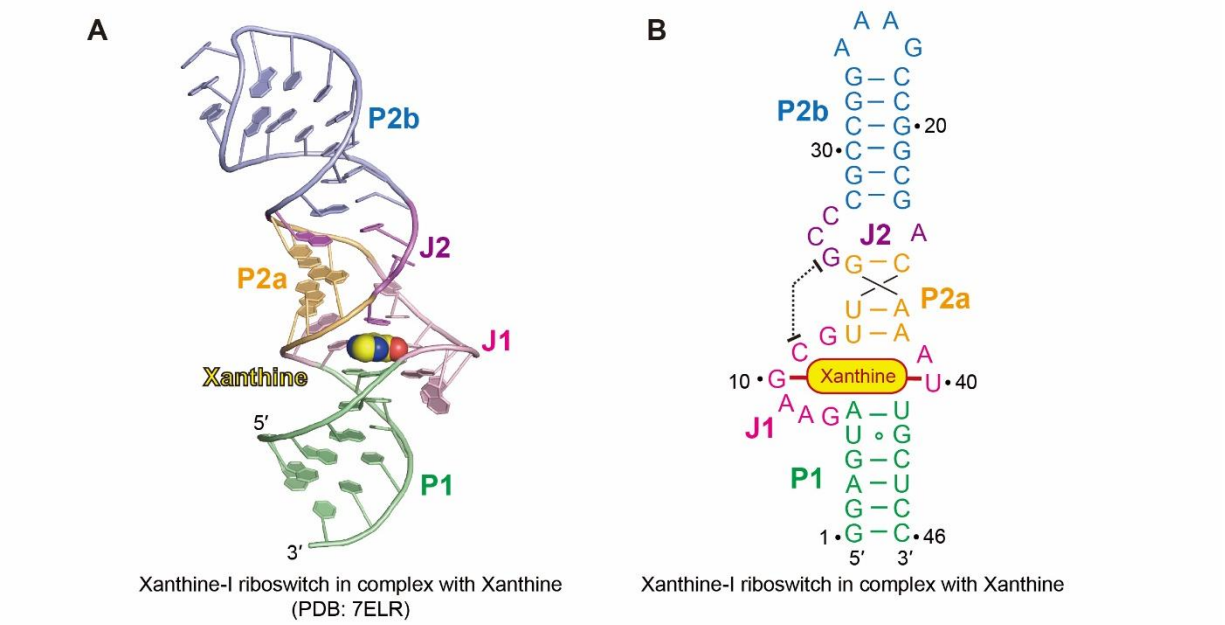

Figure S10. Tertiary Structure of xanthine-I riboswitch. A, Cartoon representation of the tertiary structure of xanthine-I riboswitch bound to xanthine (shown in spheres) (PDB:7ELR). **B,** Schematic representation of the tertiary structure of xanthine-I riboswitch, same colour code as the cartoon representation is used.

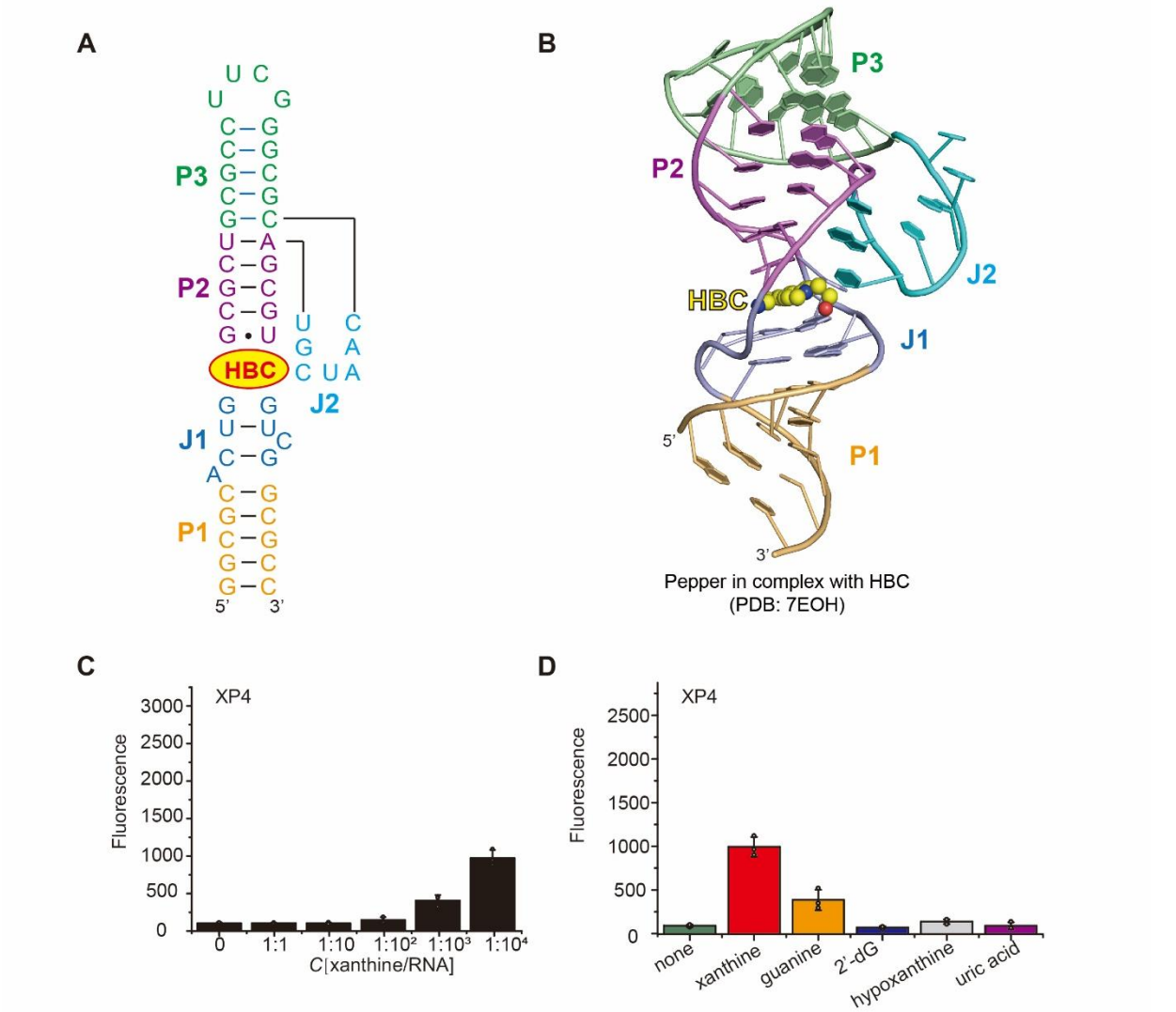

Figure S11. Tertiary structure of Pepper fluorescent aptamer and xanthine biosensor design. A, Schematic representation of the tertiary structure of Pepper fluorescent aptamer. **B,** Cartoon representation of the tertiary structure of Pepper fluorescent aptamer bound to HBC (shown in spheres) (PDB:7EOH). **C,** Fluorescence intensity of XP4 with different concentration xanthine varying from 0.1 μmol L^{-1} to 1 mmol L^{-1}. The fluorescence of XP4 is brighter with the increased xanthine concentration. **D,** Fluorescence intensity of XP4 with different purine molecules, including xanthine, guanine, 2'-dG, hypoxanthine and uric acid. XP4 exhibit a strong fluorescence response to xanthine and a slight response to guanine.

Reference：

Hamal Dhakal, S., Panchapakesan, S.S.S., Slattery, P., Roth, A., and Breaker, R.R. (2022). Variants of the guanine riboswitch class exhibit altered ligand specificities for xanthine, guanine, or 2'-deoxyguanosine. Proc Natl Acad Sci U S A 119, e2120246119.